Optimization of Parameters to Improve Ventilation in Underground Mine Working using CFD

A THESIS SUBMITTED IN PARTIAL FULLFILLMENT OF THE

REQUIREMENTS FOR THE DEGREE OF

Master of Technology

In

Mining Engineering

By

VISHAL CHAUHAN

212MN1464

DEPARTMENT OF MINING ENGINEERING

NATIONAL INSTITUTE OF TECHNOLOGY

ROURKELA – 769008

May, 2014

Optimization of Parameters to Improve Ventilation in Underground Mine Working using CFD

A THESIS SUBMITTED IN PARTIAL FULFILLMENT OF THE REQUIREMENTS FOR
THE DEGREE OF

MASTER OF TECHNOLOGY

IN

MINING ENGINEERING

BY

VISHAL CHAUHAN

212MN1464

Under the Guidance of

DR. SNEHAMOY CHATTERJEE

ASSISTANT PROFFESSOR

DEPARTMENT OF MINING ENGINEERING

NATIONAL INSTITUTE OF TECHNOLOGY

ROURKELA-769008

2013-2014

National Institute of Technology
Rourkela

CERTIFICATE

This is to certify that the thesis entitled **"Optimization of Parameters to Improve Ventilation in Underground Mine Working using CFD"** submitted by Vishal Chauhan (RollNo.212mn1464) in partial fulfillment of the requirements for the award of Master of Technology degree in Mining Engineering at the National Institute of Technology, Rourkela is an authentic work carried out by him under my supervision and guidance.

To the best of my knowledge, the matter embodied in the thesis has not been submitted to any other University/Institute for the award of any Degree or Diploma.

Date:

Dr. Snehamoy Chatterjee
Assistant Professor
Department of Mining Engineering
National Institute of Technology
Rourkela – 769008

ACKNOWLEDGEMENT

I wish to express our deep sense of gratitude and indebtedness to Dr. Snehamoy Chatterjee, Assistant Professor, Department of Mining Engineering, NIT Rourkela; for introducing the present topic and for his inspiring guidance, constructive and valuable suggestion throughout this work. His able knowledge and expert supervision with unswerving patience fathered our work at every stage, for without his warm affection and encouragement, the fulfillment of the task would have been very difficult.

We would also like to convey our sincere thanks to the faculty and staff members of Department of Mining Engineering, NIT Rourkela, for their help at different times.

Last but not least, our special thanks to my friends who have patiently extended all sorts of help for accomplishing this project.

Date:

VISHAL CHAUHAN

212MN1464

Department of Mining Engineering

CONTENTS

Certificate iii

Acknowledgement iv

Abstract vii

List of Figures viii

List of Tables ix

Chapter1: Introduction **1**

1.1 Overview 2

1.2 Mine Ventilation 2

1.3 Computational Fluid Dynamics (CFD) 3

1.4 Optimize the brattice location 4

1.5 Objectives 5

Chapter2: Literature Review **6**

2.1 Overview 7

2.2 Literature survey 7

Chapter3: Methodology **12**

3.1 Overview 13

3.2 Problem Identification 14

3.2.1 Define goals 14

3.2.2 Identify domain 14

3.3 Pre-Processing 14

3.3.1Geometry (Model Development) 14

3.3.2 Mesh 16

3.3.3 Setup (physics) and Solver setting 18

3.3.3.1 Assumptions 18

3.3.3.2 Governing equations 18

3.3.3.3 Setup data 21

3.4 Objectives and Optimization Methods 22

3.4.1 Objectives Requirements According to Optimization Method …..……... 22
3.4.2 Screening approach ……...…….24
3.4.3 MOGA approach ……... 25
3.4.4 NLPQL approach ……...……... 26

Chapter4: Results and Discussion ……...……... 28
4.1 Overview …….…… 29
4.2 Solution …… 29
4.3 Simulation Results …….……..…… 29
4.4 Correlation between Input Parameter and Velocity ……...…...……... 39

Chapter5: Conclusion ……...……... 42
5.1 Conclusion …… 43

Chpater6: References……...……. 44
6.1 References ……...……. 45

ABSTRACT

In underground mine, it is very important to maintain fresh and sufficient air in unventilated areas to maintain safe working environment for workers. To study the behaviour of air flow in underground mine, a T-shaped crosscut region of Bord and Pillar mining is considered for simulation in two different cases: without and with thin brattice positioning at crosscut region. Brattice is cost effective ventilation control device to deflect air into unventilated areas in underground mine. The ultimate objective is to find the best location and dimension of brattice across the crosscut region by which one can get maximum velocity at dead end. In this thesis, a computational fluid dynamics (CFD) and optimization algorithms are considered for maximizing the air flow at the dead end by placing a brattice at optimum location. Two different optimization algorithms: multi-objective genetic algorithm (MOGA) and non-linear programming of quadratic Lagrangian (NLPQL) optimization techniques were used in this study. ANSYS FLUENT software is used for CFD modeling at T-shaped crosscut region and computes the simulation result of air flow velocity at dead end. Optimization techniques are used for to optimize four input parameters; brattice position vertical and horizontal from the wall of crosscut region and width and length of brattice. The objectives for optimizations are to maximize the velocity at dead end and minimize the pressure drop in crosscut region. Comparison is carried out between crosscut region without and with a thin brattice using optimization techniques and found the best location and dimension of brattice. To increase the air flow velocity at dead end increases the safe working for workers and supply adequate air at working face.

List of Figures

Figure 3.1 A CFD solver steps to solve a problem

Figure 3.2 T-shaped crosscut region without Brattice (3D view)

Figure 3.3 T-shaped crosscut region with Brattice (2D view)

Figure 3.4 Meshed crosscut region with no brattice

Figure 3.5 Meshed crosscut region with brattice

Figure 3.6 Sample chart prepared by the Screening optimization technique

Figure 3.7 Sample chart prepared by the MOGA optimization technique

Figure 3.8 Sample chart prepared by the NLPQL optimization technique

Figure 4.1 Velocity Contour of T-shaped crosscut region without brattice

Figure 4.2 Pressure Contour of T-shaped crosscut region without brattice

Figure 4.3 Velocity Contour of T-shaped crosscut region with thin brattice

Figure 4.4 Pressure Contour of T-shaped crosscut region with thin brattice

Figure 4.5 Velocity Contour of T-shaped crosscut region with thin brattice by MOGA optimization

Figure 4.6 Pressure Contour of T-shaped crosscut region with thin brattice by MOGA optimization

Figure 4.7 Velocity Contour of T-shaped crosscut region with thin brattice by NLPQL optimization

Figure 4.8 Pressure Contour of T-shaped crosscut region with thin brattice by NLPQL optimization

Figure 4.9 Relation between Brattice position vertical and Velocity

Figure 4.10 Relation between Brattice position horizontal and Velocity

Figure 4.11 Relation between Brattice width and Velocity

Figure 4.12 Relation between Brattice length and Velocity

List of Tables

Table 3.1 Dimension of geometry parts

Table 3.2 Input Parameters for optimization

Table 3.3 Input data for simulation

Table 3.4 Output Parameters for optimization

Table 3.5 Optimization domain of input parameters

Table 3.6 Optimization objective for screening approach

Table 3.7 Optimization objective for MOGA approach

Table 3.8 Optimization objective for NLPQL approach

Table 4.1 Final result in case of crosscut region with no brattice

Table 4.2 Final result in case of crosscut region with brattice

Table 4.3 Optimized result by MOGA approach

Table 4.4 Optimized result by NLPQL approach

Chapter1. Introduction

1.1 Overview

Coal, a combustible fossil fuel, is an important resource for electricity generation. It is mined from underneath the ground where a coal stratum is present. Coal originates from terrestrial land plants buried under increased heat and pressure from millions of years ago. The land plants decompose to become an organic chemical compound which eventually becomes coal after further heating in a process known as digenesis (Amano et al. 1987). The extraction of coal is generally done by either open pit or underground method. When the depth of the coal deposit is relatively high, the underground mining method is preferred. However, underground mine is associated with large amount of risk mainly due to gas and coal dust explosion.

To reduce the risk associated with underground mining, efficient and adequate ventilation is preferred. Improving the amount of air ventilation would improve the level of safety in coal mines. Efficient and adequate ventilation would reduce the possibility of explosion by mitigating the amount of dangerous gases present by aiding airflow and preventing recirculation.

1.2 Mine Ventilation

In underground mining, it is of particular importance to maintain fresh and cool air in unventilated areas to maintain safe working environments for workers inside a coal mine. The underground mining environment is subjected to the dangers of heating due to excess oxygen as well as presence of dangerous gases such as methane. As a result, air is injected into underground mines as a way to ventilate the surrounding air. This serves to dilute as well as reduce the air temperature in the mine. By hanging as simple a device as a brattice sail, as air is injected into a mine, brattice sails can be aid the airflow into unventilated areas and bring contaminants out of the region.

Aminossadati and Hooman (2008) compared the different lengths of brattices and their effectiveness with regard to their length into the crosscut region. In their study, it is noted that with brattices lengths up to entire length of the cross-cut region proved to be most effective. However, the brattice lengths were only confined to a simple cross-cut region in their study. This proves to be a limitation as coal mine is filled with many rooms and pillars. Brattice sails would enable better airflow as cool air would reach unventilated areas for a safer

working environment. A study has analyzed the airflow pattern in working faces and concluded that the usage of a brattice is mandatory in preventing recirculation and to control respiratory dust in the face area.

An inclusion of a brattice sail would successfully dispose unwanted contaminants out of these regions. Cross cut regions in coal mines typically house mining equipment, various machineries and electrical equipment such as transformers. Most miners will not frequent such areas, but it is important to analyze these regions so as to make them save for those that do.

In mine ventilation, to analyze the fluid flow through these cross-cuts and network, the commonly used method is Hardy-Cross method. The main limitation of this algorithm is that it over simplified fluid dynamics problem by assuming number of parameters constants.

In this thesis, the problem of mine ventilation is solved by computational fluid dynamics (CFD). Computational fluid dynamics is the science of predicting fluid flow analysis complements testing and experimentation by reducing total effort and cost required for experimentation and data acquisition.

1.3 Computational Fluid Dynamics (CFD)

Computational Fluid Dynamics (CFD) is the simulation of fluids engineering systems using modeling (mathematical physical problem formulation) and numerical methods (discretization methods, grid generations solvers, and numerical parameters etc). To solve the fluid problem, the physical and chemical properties of fluid should be known. Then mathematical equations are used to describe these physical properties. This is Navier-Stokes Equation and it is the governing equation of CFD. As the Navier-Stokes Equation is analytical, human can understand it and solve them on a piece of paper. But for solving these problems by computer, translate the problem into the discretized form. The translators are numerical discretization methods, such as Finite Difference, Finite Element, Finite Volume methods. Consequently, whole problem is dividing into many small parts because discretization is based on that. At the end, simulation results are obtained. If the problem consist the turbulent flow then there are some turbulent models are also used during CFD analysis as following (Kurnia et al. 2014)

1. Spalart-Allmaras model

2. *k*-ε models

3. *k*-ω models

4. Reynolds stress model (RSM)

Turbulent flows in fluids consist of fluctuating velocity fields. These fluctuations are caused by the interaction of energy, momentum, and transported entities and species concentration in the fluid.

1.4 Optimize the brattice location

The purpose of underground mine ventilation is to supply sufficient amount of air at the working face. To maximize the air at the working face, brattices are generally used. The locations of the brattice play an important role for maximizing the flow at working faces. The goal driven optimization can be used couple with CFD, to optimize the location of the brattices.

Goal Driven Optimization (GDO) is a set of constrained, multi-objective optimization (MOO) techniques in which the "best" possible designs are obtained from a sample set given the goals set for parameters. There are three available optimization methods: Screening, Multi-Objective Genetic Algorithm (MOGA), and Non-Linear Programming by Quadratic Lagrangian (NLPQL). MOGA and NLPQL can only be used when all input parameters are continuous.

The GDO process allows determining the effect on input parameters with certain objectives applied for the output parameters. GDO can be used for design optimization in three ways: the Screening approach, the MOGA approach, or the NLPQL approach. The Screening approach is a non-iterative direct sampling method by a quasi-random number generator based on the Hammersley algorithm. The MOGA approach is an iterative Multi-Objective Genetic Algorithm, which can optimize problems with continuous input parameters. NLPQL is a gradient based single objective optimizer which is based on quasi-Newton methods.

The GDO framework uses a decision support process based on satisfying criteria as applied to the parameter attributes using a weighted aggregate method. In effect, the DSP can be

viewed as a post processing action on the Pareto fronts as generated from the results of the MOGA, NLPQL, or Screening process.

Usually the Screening approach is used for preliminary design, which may lead you to apply the MOGA or NLPQL approaches for more refined optimization results.

1.5 Objectives

Coal mining ventilation is a broad subject. This project covers a specific section i.e., ventilation in a crosscut region or T-section in a Bord and Pillar mine. This project addresses the ventilation of mines from a modeling and simulation point of view. The models are drawn and meshed on ANSYS software, and subsequent Computational Fluid Dynamics (CFD) analysis is implemented using FLUENT Software. For CFD analysis, a turbulence Spalart-Allmaras model is used.

For simulation, a thin brattice for a variety of added scenarios are used in this thesis. The width, length of brattice and position of brattice from crosscut region to wall are varied. In subsequent, changes to the modeling structure are implemented to improve the accuracy of the experiment. After the CFD analysis, the optimization theory like Multi-Objective Genetic Algorithm (MOGA) and Non-Linear Programming by Quadratic Lagrangian (NLPQL) to get the best result according to input parameters and get best output parameters i.e., velocity at dead end i.e. working faces and pressure drop across T-section.

In this simulation study, the air flow velocity at dead end or working face of crosscut region and pressure drop in this region are analyzed. The main objective of this thesis is to optimize the brattice location by calculating the different parameters like brattice position in crosscut region and the width, length of brattice inside a crosscut region to aid in airflow using fluent, a CFD program and optimization algorithm. The simulations will be basic tests on the fluid flow behavior with brattice sails. The ultimate objective is to find best location and dimension of brattice across the crosscut region that could get maximum velocity at dead end.

Chapter2. Literature Review

2.1 Overview

An exhaustive literature survey has been carried out on mine ventilation and CFD analysis of the flow properties in an underground working area. The research and studies on this field started a long back. A few of this research works is presented in this chapter. The review can be separated into various modules or sub-reviews such as experimental studies, theoretical studies and numerical studies. Based on this important review papers, scope and objective of the present study is established.

This chapter gives an insight into the present state of knowledge about the flow characteristics in underground mine by exploring the available literature. This has also helped to decide the scope of the present study.

2.2 Literature Survey

Kurnia et al. (2014) developed a mathematical model for methane dispersion in an underground mine tunnel with discrete methane sources and various methods to handle it, utilizing the CFD approach. The study provided some new ideas for designing an ‘‘intelligent’’ underground mine ventilation system which can cost-effectively maintain methane concentration below the critical value. It also highlighted the importance of methane monitoring to detect locations of methane source for effective control of methane concentration for designing an effective mine ventilation system.

Chanteloup and Mirade (2009) reported the implementation of the ‘‘age of air” concept into commercial CFD code Fluent through user define function (UDF) to assess ventilation efficiency inside forced-ventilation food plants using two transient methods and the steady-state method. The results indicated that calculating local mean age of air (MAA) by steady-state method proved the best compromise between accuracy of results and computation time.

Toraño et al. (2011) presented a study of dust behavior in two auxiliary ventilation systems by CFD models, taking into account the influence of time. The accuracy of these models was assessed and validated by measurement of airflow velocity and respirable dust concentration taken in six points of six roadways in an operating coal mine. It was concluded, that the predictive models allowed modification of auxiliary ventilation and improved health conditions and productivity.

Diego et al. (2011) calculated the losses in 138 situations of circular tunnels, varying tunnel diameter, air velocity and surface characteristics, by both traditional and CFD means. The results of both methods were compared and adequate correlation was observed with CFD values constant at 17% below the values calculated by traditional means.

Xu et al. (2013) conducted a laboratory experiment using tracer gas methodology in conjunction with CFD studies to examine the ventilation status of a mine after an incident. A laboratory model mine was built based on a conceptual mine layout which allowed changes to the ventilation status to simulate different ventilation scenarios after an incident. SF_6 was used as tracer gas and different gas sampling methods were evaluated. A gas chromatograph equipped with an electron capture detector was used for analyzing the gas samples. The results indicated that tracer gas concentrations can be predicted using CFD modeling and different ventilation statuses will result in substantially different tracer gas distribution.

Sasmito et al. (2013) carried out a computational study to investigate flow behavior in a ‘‘room and pillar’’ underground coal mine. Several turbulence models, Spallart–Almaras, k-Epsilon, k-Omega and Reynolds Stress Model, were compared with the experimental data from Parra et al. (2006). The Spallart–Almaras model was found to be sufficient for prediction of flow behavior adequately in underground environment whilst keeping low computational cost.

Torno et al. (2013) carried out a study in a deep underground mine located in Northern Spain, by measurements of blasting gases, CO and NO_2, in three cross-sections of the coal heading located at 20, 30 and 40 m from the heading face. Mathematical models of gas dilution were developed according to the dilution time after blasting. The obtained values by the experimental models and the values of other mathematical models showed differences, which indicated the need to obtain in each underground work its own dilution models of blasting gases.

Ren et al. (2014) conducted a study to investigate both airflow and respirable dispersion patterns over the bin and along the belt roadway to design a better dust mitigation system. The results showed the dispersion of airborne dust particles from the underground bin dictated by the ventilation airflow pattern distributed widely in the belt roadway and at various elevations above the floor, contributing to high dust contamination of intake air. CFD modeling results showed that ventilation from the horizontal intake at a rate of 10–13 m^3/s would help dilute and confine the majority of dust particles below the workers’ normal

breathing zone. An innovative dust mitigation system based on the water mist technology was also proposed. The feasibility of the new system on respirable dust control was investigated and verified from a theoretical perspective followed by a detailed design, which was approved for field implementation.

Kurnia et al. (2014) conducted a parametric study in an underground mine to investigate effects of various factors influencing the effectiveness and performance of novel intermittent ventilation system for air flow control. It was found that intermittent ventilation could reduce electrical energy consumption by 25% compared to steady flow ventilation, whilst maintaining methane level in the mining face below the allowable level.

Guo and Zhang (2014) presented a new integral theory for tunnel fire under longitudinal ventilation. The solution on critical velocity was compared with experimental data and the results of CFD simulation from two different computer programs. The comparison showed that general agreement among the data was satisfactory. The trend of variation for critical velocity versus fire size shown in the experimental data was confirmed by both theoretical and CFD predictions.

Aminossadati and Hooman (2008) studied about behavior of fluid flow in underground mine by using CFD. They simulated CFD modeling to know the behavior of airflow in underground mine. They also described airflow behavior in underground crosscut region. In crosscut region of underground mine, they established brattice. Brattice is used for direct the airflow in that region and brattice is ventilation control device for permanent or temporary use in underground mine. Brattice can be used to deflect air into the unventilated areas such as crosscut regions. In their study, they compare the effects of brattice length on fluid flow behavior in the crosscut regions and present the 2D CFD model.

Torano et al. (2011) described dust behavior by CFD models in two auxiliary ventilation systems with respect to the time. The accuracy of CFD models assessed by airflow velocity and respirable dust concentration measurements in coal mine. They concluded the CFD models allow optimization of the auxiliary ventilation system calculated by conventional methods.

Likar and Cedez (2000) proposed an alternative approach to the ventilation design of enclosed and half-enclosed underground structures where more analysis is required. They

showed the advantage of such an approach a calculation of movement of exhaust air through an enclosed structure as a function of time.

Lowndes et al. (2004) has described climate and ventilation modeling of tunnel. They detailed the results of a series of correlation and validation studies conducted against the climate survey and ventilation data. They illustrated the basics of airflow behavior in rapid development of tunnel.

Ghosh et al. (2013) has explained ventilation in Bord and Pillar underground mine using CFD. Their ultimate objective is to design a system that is capable of ventilating all airways, working faces and areas underground at minimum cost. They examines the airflow pattern in mine ventilation system in Bord and pillar system of mining with the help of two-dimensional computational fluid dynamics modeling.

Parra et al. (2006) has found that ventilation plays an essential role in underground working. They studied ventilation working systems by numerical and experimental sense. They setup a real mine gallery and measurements taken with a hot-wire anemometer. They described air flow behavior in three types of ventilation system: exhaust, blowing and mixed ventilation.

Torano et al. (2009) studied about ventilation modeling and behavior of methane in underground coal mine using CFD. They measured methane concentration and airflow velocity. They compared the results obtained by conventional method with results obtained by CFD modeling. They found that CFD modeling allows us to know in which zones it may be necessary to forcing ventilation such as jet fans, exhaust ventilation, spray fan or compressed air injectors.

Su et al. (2008) has explained air flow characteristics of coal mine ventilation. They focused on methane emission from underground mine, in particular ventilation air methane capture and utilization. They also discussed possible correlation between ventilation air characteristics and underground mine activities.

Hargreaves and Lowndes (2007) illustrated the computational modeling of ventilation flows with in rapid development drivage. They constructed the CFD models of ventilation flow patterns during the bolting and cutting cycle. They concluded the CFD models may be successfully used to identify the ventilation characteristics associated with the various auxiliary systems.

Liu et al. (2009) presented ventilation simulation model on multiphase flow in mine. They setup a 3D mathematical model of working face by using computational fluid dynamics (CFD) and simulated heat exchange of multiphase flow in ventilation pipeline. They stated the changing of one phase into the other phase.

Collela et al. (2011) stated that transient Multiscale modeling from ventilation and fire in long tunnels. They coupled transient model with CFD solver with 1D network model. In tunnel regions, flow is fully developed but CFD models require near field. They illustrated numerical models to the discussion of algorithm of coupling. Their methodology is applied to study the transient flow interaction between a growing fire and ventilation system. The results allowed for simultaneous optimization of the ventilation and detection systems.

Amano et al. (1987) proposed that a new method for calculating underground air moisture. As there are problems associated with obtaining specific resistance and elapsed time factor for each airway, such as estimating these factors, author has come out with a system to calculate the underground air moisture.

Noack et al. (1998) studied on method to predict gas emission in coal mines. According to the author, there is a formula to calculate an air requirement. They also proposed a few ventilation solutions such as introducing an auxiliary fan as well as using a gas drainage borehole to reduce emission.

Kissell and Matta (1979) investigated use of line brattice in coal mines. They found that line brattice aids airflow into dead zones.

Chapter3. Methodology

3.1 Overview

In this thesis, a T-shaped crosscut region of Bord and Pillar mining in underground mine for ventilation simulation is used. The ventilation simulation was performed by computational fluid dynamics modeling. For CFD analysis, ANSYS software is used. FLUENT is the ANSYS solver to solve the fluid related problems. The solver is based on Finite Volume method. Before CFD simulation, domain is discretized into a finite set of control volumes.

There are some steps to solve ventilation simulation as following –

1. Problem identification

2. Pre-Processing

3. Solution

4. Post-Processing

Figure 3.1 represents different steps of solving ventilation simulation using CFD analysis.

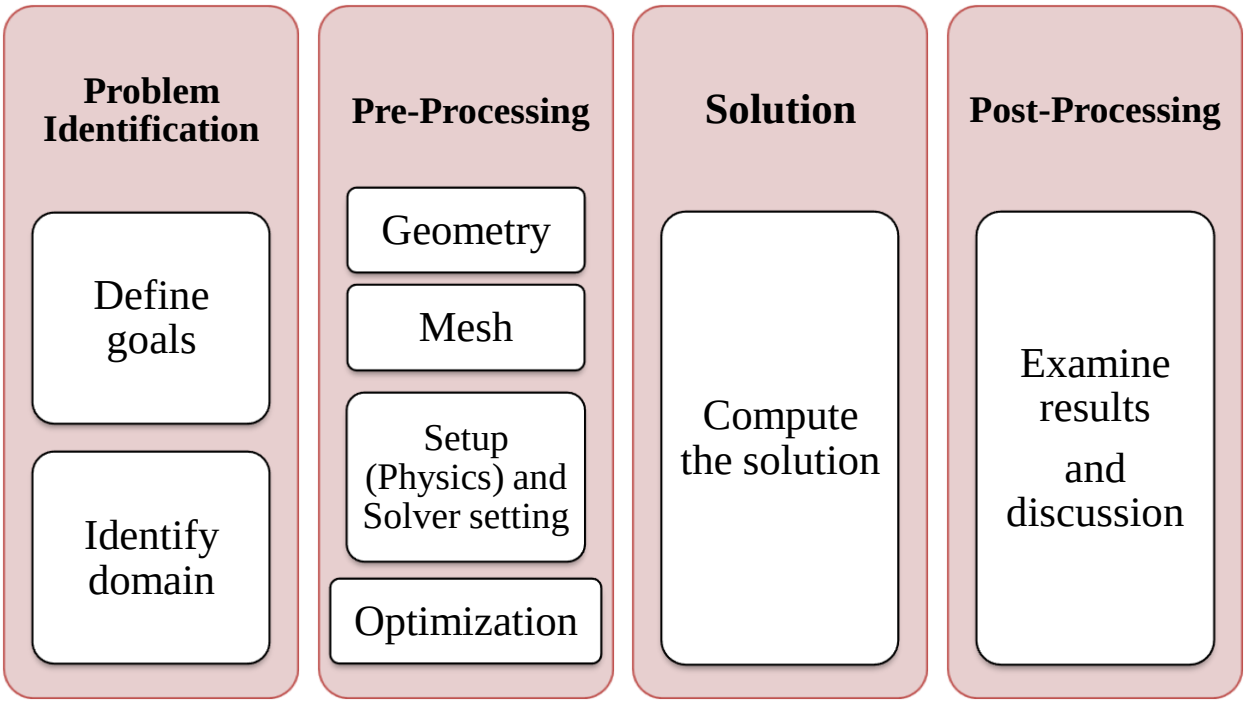

Figure 3.1 A CFD solver steps to solve a mine ventilation problem

3.2 Problem Identification

3.2.1 Define goals - In this section, the goals according to the problem are identified. The ultimate objective is to get maximum velocity at the dead end and minimize the pressure drop across the crosscut region.

3.2.2 Identify domain – In this section, we identify the domain of our problem. In T-shaped crosscut region, we identify different domain like inlet, outlet, dead end or working face, brattice etc.

3.3 Pre-Processing

In Pre-processing section, the geometry of the underground mine ventilation cross-cut is developed using ANSYS design module. The domain is discretized or meshed into many finite domains by mesh module. After the meshing, the mine ventilation system is simulated by FLUENT solver. The solver parameters are set according to fluid model, material, properties, boundary conditions, solving techniques, turbulence model, convergence criterion etc. For optimization purpose, the objective is maximized i.e. the velocity at dead end and pressure drop is minimized within the constrained bound. To calculate the objective function values within the constrained domain, FLUENT solver is called for simulating those values.

3.3.1 Geometry (Model Development)

3D models of T-shaped crosscut region without brattice and with brattice are prepared and presented in Figure 3.2 and Figure 3.3, respectively. The geometry is created to reflect the actual underground mine cross-cut.

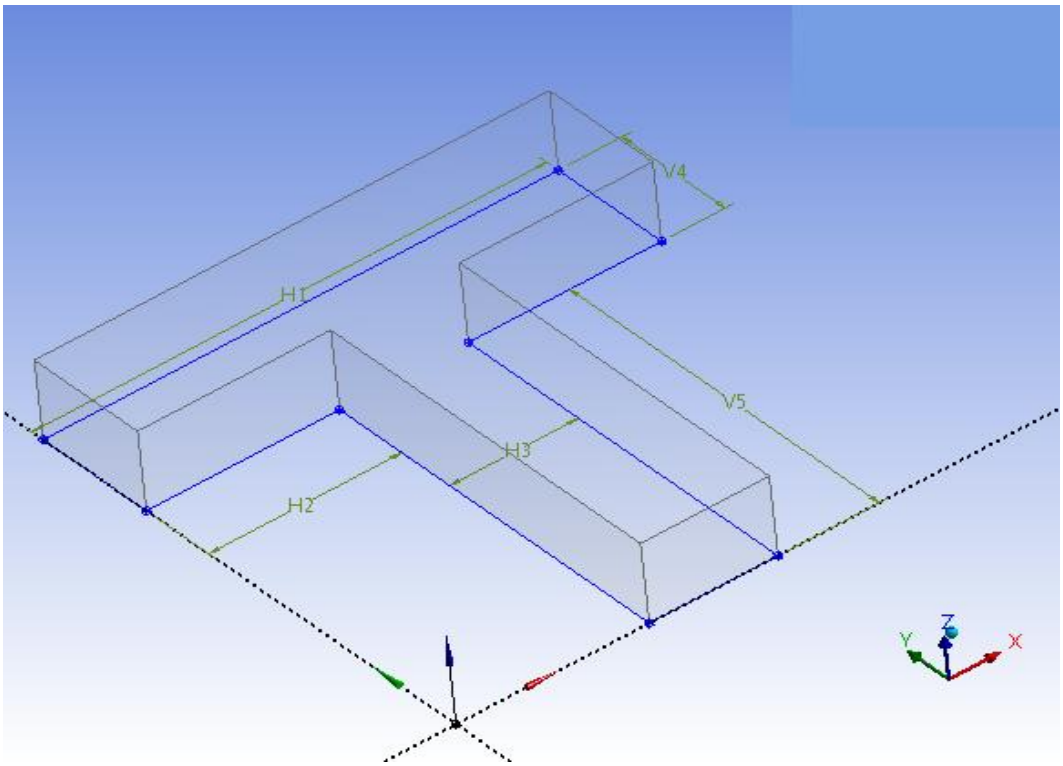

Figure 3.2 T-shaped crosscut region without Brattice (3D view)

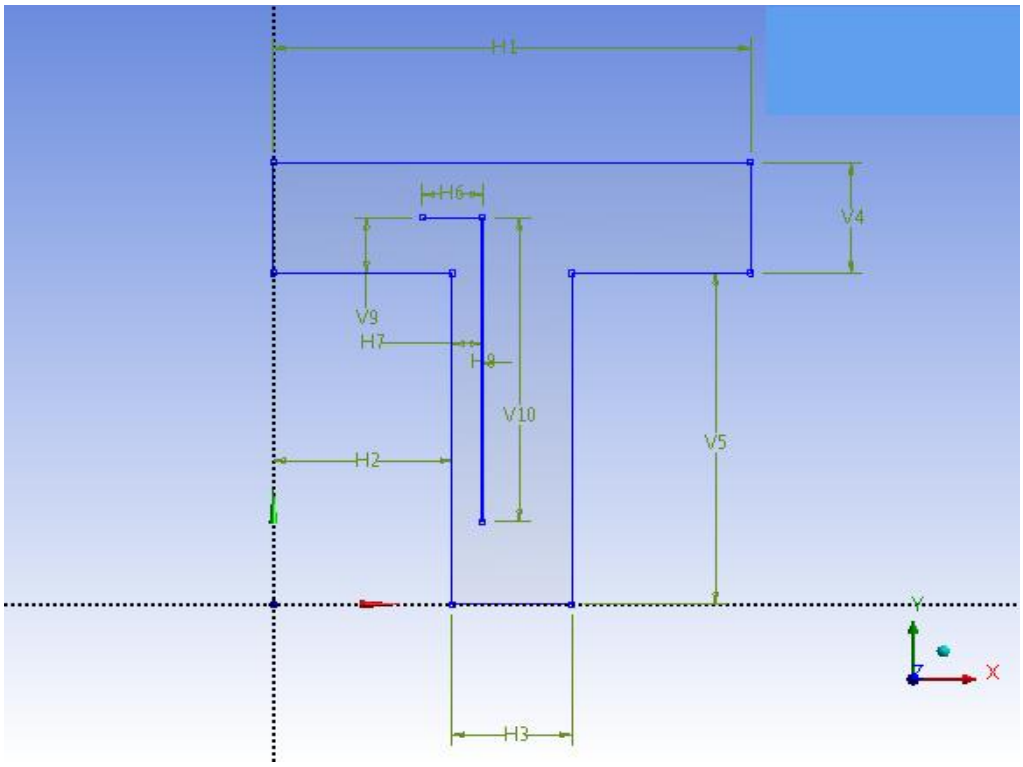

Figure 3.3 T-shaped crosscut region with Brattice (2D view)

The dimension of crosscut region and ventilation is following in Table 3.1. For normal case, it was considered that the brattice width, brattice length, brattice position vertical, and brattice position horizontal are known. However, during optimization, those values are selected to maximize the velocity at the dead end.

Table 3.1 Dimension of geometry parts

Geometry Parameter	Name	Value (meter)
H1	T-section width	16 m
H2	Crosscut region distance	6 m
H3	Crosscut width	4 m
V4	T-section Length	4 m
V5	Crosscut Length	12 m
H6	Brattice width	2 m
V10	Brattice length	11 m
V9	Brattice position vertical	2 m
H7	Brattice position horizontal	1 m

After creating the geometry, four input parameters for optimization by which one can get maximize the velocity at dead end and minimize the pressure drop are identified and presented in Table 3.2 shows the input parameters for optimization.

Table 3.2 Input Parameters for optimization

Sl. No.	Parameter	Parameter Name
1.	V9	Brattice Position Vertical
2.	H7	Brattice Position Horizontal
3.	H6	Brattice Width
4.	V10	Brattice Length

3.3.2 Mesh

In mesh section, geometry is imported into the ANSYS mesh module and performs a fine meshing size to both the geometries of T-shaped with no brattice and with brattice as shown Figure 3.4 and Figure 3.5, respectively.

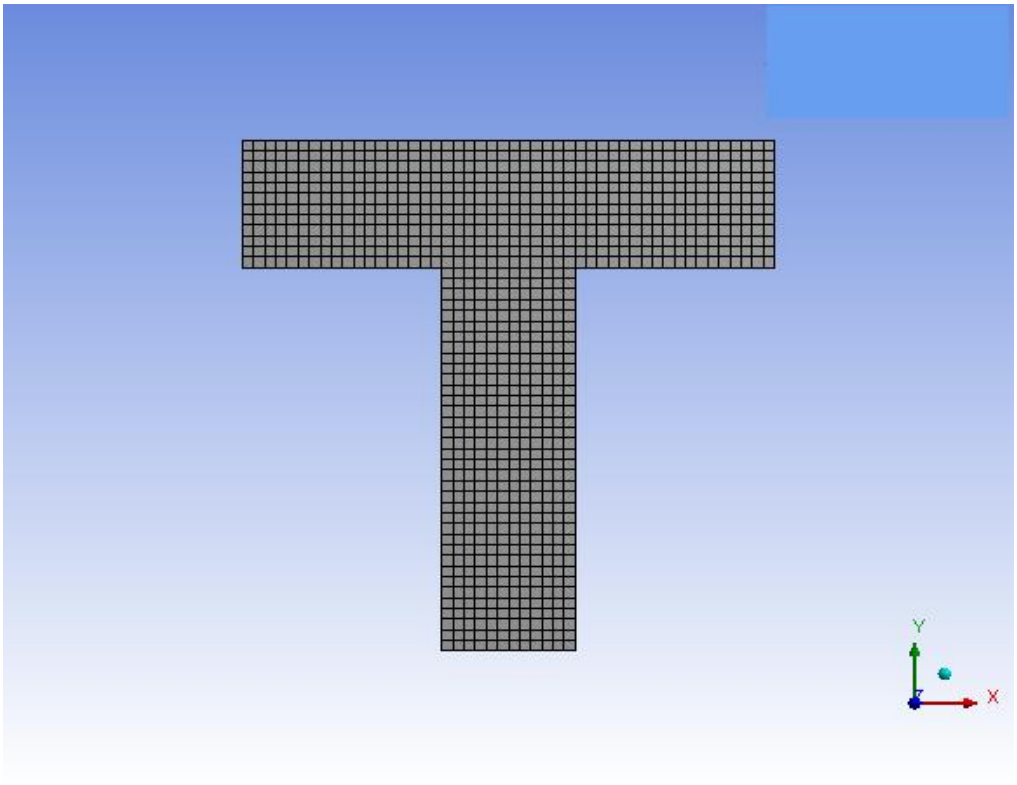

Figure 3.4 Meshed crosscut region with no brattice

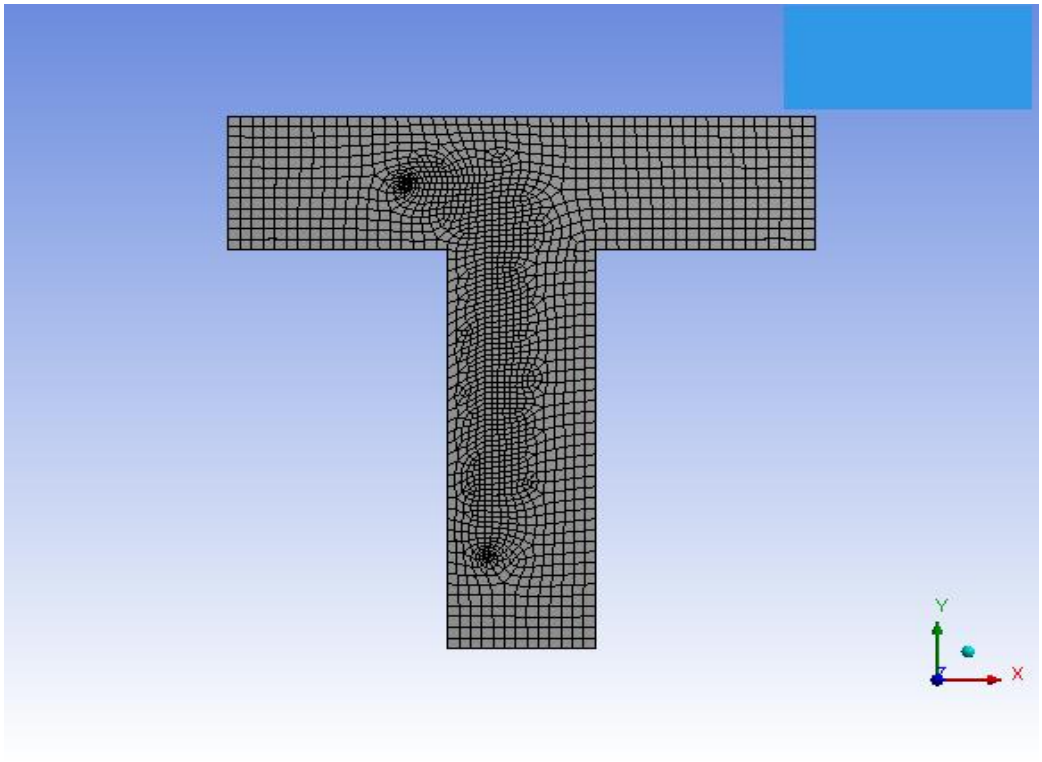

Figure 3.5 Meshed crosscut region with brattice

3.3.3 Setup (Physics) and Solver setting

After the meshing, mesh part of geometry was imported into the setup of software. First, mesh and mesh quality were checked; if meshing is not been well performed then there will be an error.

3.3.3.1 Assumptions

There are some assumptions regarding our problem as following –

1. The walls of the crosscut regions are assumed to be smooth.
2. The air is assumed to be at room temperature.
3. Air is an incompressible fluid.
4. Mine ventilation is independent of time i.e. steady-state process.
5. Neglect the stress tensor and body force.

3.3.3.2 Governing Equations

The governing equation of computational fluid dynamics (CFD) is known as Navier-Stokes equations. Navier-Stokes equations consist of conservation of mass, momentum, energy, species etc equations. The governing equations are following

Conservation equation of mass

$$\frac{\partial \rho}{\partial t} + \nabla.(\rho V) = 0$$

where, ρ is the air density and V is the air velocity.

Conservation equation of momentum

$$\frac{\partial \rho V}{\partial t} + \nabla.(\rho V V) = -\nabla \mathbf{p} + \nabla.\bar{\bar{\tau}} + \rho g$$

where, ρ is the air density, V is the air velocity, $\mathbf{p}$ is the pressure force, $\bar{\tau}$ is stress tensor and g is the gravitational force.

Turbulent model equation

The Spalart-Allmaras turbulent model was used for this experiment. The governing equation for this model is:

$$\boldsymbol{\nabla.(\rho\tilde{\nu}V) = G_{\nu} + \frac{1}{\sigma_{\nu}}\left[\nabla.(\mu+\rho\tilde{\nu})\nabla\tilde{\nu} + C_{b_2}\rho(\nabla\tilde{\nu})^2\right] - Y_{\nu}}$$

where, G_ν is the production of turbulent viscosity, Y_ν is the destruction of turbulent viscosity, σ_ν and C_{b_2} are the constants, ν is the kinematic viscosity and $\tilde{\nu}$ is the turbulent kinematic viscosity.

The turbulent dynamic viscosity μ is computed from

$\mu = \rho\tilde{\nu}f_{v_1}$

where, the viscous damping function, f_{v_1} is given by

$f_{v_1} = \frac{\chi^3}{\chi^3 + C_{v_1}{}^3}$ and $\chi = \frac{\tilde{\nu}}{\nu}$

The production term, G_ν is modeled as –

$G_\nu = C_{b_1}\rho\tilde{S}\tilde{\nu}$

where, $\tilde{S} = S + \frac{\tilde{\nu}}{k^2d^2}f_{v_2}$ and

$$f_{v_2} = 1 - \frac{\chi}{1 + \chi f_{v_1}}$$

where, C_{b_1} and k are constants, d is the distance from the wall, and S is a scalar measure of deformation tensor which is based on the magnitude of the vorticity.

$S = |\Omega_{ij}| + C_{prod}\min(0, |S_{ij}| - |\Omega_{ij}|)$

where, Ω_{ij} is the mean rate of rotation tensor and S_{ij} is the mean strain rate, defined by

$|\Omega_{ij}| = \frac{1}{2}\left(\frac{\partial V_i}{\partial x_j} - \frac{\partial V_j}{\partial x_i}\right)$, $S_{ij} = \frac{1}{2}\left(\frac{\partial V_j}{\partial x_i} + \frac{\partial V_i}{\partial x_j}\right)$,

and $|\Omega_{ij}| = \sqrt{2\Omega_{ij}\Omega_{ij}}$, $C_{prod} = 2$, $S_{ij} = \sqrt{2S_{ij}S_{ij}}$

Including both rotation and strain tensor reduces the production of eddy viscosity and consequently reduces the eddy viscosity itself in regions where the measure of vorticity exceeds that of strain rate.

The destruction term,Y_v modeled as

$$Y_v = C_{w_1}\rho f_w \left(\frac{\tilde{\nu}}{d}\right)^2$$

where,

$$f_w = g\left[\frac{1 + {C_{w_3}}^6}{g^6 + {C_{w_3}}^6}\right]^{1/6}$$

$$g = r + C_{w_2}(r^6 - r)$$

$$r = \frac{\tilde{\nu}}{\tilde{s}k^2d^2}$$

where, $C_{w_1}, C_{w_2} and\ C_{w_3}$ are constants.

The model constants have the following values,

$$C_{b_1} = 0.1355,\ C_{b_2} = 0.622,\quad \sigma_{\tilde{\nu}} = \frac{2}{3},\quad C_{v_1} = 7.1$$

$$C_{w_1} = \frac{C_{b_1}}{k^2} + \frac{\left(1 + C_{b_2}\right)}{\sigma_{\tilde{\nu}}}, C_{w_2} = 0.3, C_{w_3} = 2, k = 0.4187$$

Governing Equations for this experiment

The governing equations for this experiment (Single Phase flow) is

$$\frac{\partial \rho \Phi}{\partial t} + \nabla(\rho V \Phi) - \nabla(\Gamma_\Phi grad\ \Phi) = S_\Phi$$

where, Φ is the output parameter i.e. velocity at dead end, ρ is the air density and *V* is the inlet velocity, Γ_Φ is the diffusive coefficient and S_Φ is the source rate per unit volume. In this experiment, diffusive and source term is absent.

3.3.3.3 Setup data

For simulation purpose, some date like fluid material, solver, turbulent model, boundary conditions, solution method, convergence criterion etc are assumed to be known. Table 3.3 shows the input data according to problem and what we want in results.

Table 3.3 Input data for simulation

Solver	Pressure-Based
Time	Steady
Turbulent Model	Spalart-Allmaras model
Material	Air
Operating Pressure	101325 Pa
Operating Temperature	288.16 K
Inlet Velocity	2 m/s
Convergence criterion	1E-06
Number of Iteration	1000

In final step, problem is iteratively solved till the convergence criterion is achieved. In the solver setting, the output parameters were also set. These output parameters were used for optimization purpose. Table 3.4 shows the output parameters to optimize. The output parameters are optimized to select the optimum brattice location using Goal Driven Optimization (GDO) module of ANSYS software.

Table 3.4 Output Parameters for optimization

Sl. No.	**Output Parameter Name**
1.	Velocity at dead end (V_d)
2.	Pressure drop (P_d)

3.4 Objectives and Optimization Methods

If the location of the brattice is known i.e. the values of H6, H7, V9, and V10, one can calculate the values of V_d and P_d using the CFD analysis. According to resulted value of output parameters from CFD analysis, the optimization techniques in Goal Driven Optimization in ANSYS software can be applied to select the values of H6, H7, V9, and V10.

Optimization techniques can be used for design optimization in three ways: the Screening approach, the MOGA approach, or the NLPQL approach. The Screening approach is a non-iterative direct sampling method by a Quasi-Random number generator based on the Hammersley algorithm. The MOGA approach is an iterative Multi-Objective Genetic Algorithm, which can optimize problems with continuous input parameters. NLPQL is a gradient based single objective optimizer which is based on Quasi-Newton methods. Usually the Screening approach is used for preliminary design, which may lead to apply the MOGA or NLPQL approaches for more refined optimization results.

3.4.1 Objectives Requirements According to Optimization Method -

Screening uses any goals that are defined the samples in the samples chart, but does not have any requirements concerning the number of objectives or goals defined.

MOGA requires that a goal is defined (i.e., an Objective is selected) for at least one of the output parameters. Multiple output goals are allowed. The following two objectives are fixed for MOGA

Maximize V_d

Minimize P_d

NLPQL requires that a goal is defined (i.e., an Objective is selected) for at exactly one output parameter. Only a single output goal is allowed. The following objective function is fixed for NLPQL

Maximize V_d

Screening Optimization- The Screening option is not strictly an optimization approach; it uses the properties of the input as well the output parameters, and uses the Decision Support Process on a sample set generated by the Shifted Hammersley technique to rank and report the candidate designs.

MOGA and NLPQL Optimization- When the MOGA or NLPQL optimization methods are used for Goal Driven Optimization; the search algorithm uses the Objective properties of the output parameters and ignores the similar properties of the input parameters. However, when the candidate designs are reported, the first Pareto fronts (in case of MOGA) or the best solution set (in case of NLPQL) are filtered through a Decision Support Process that applies the parameter Optimization Objectives and reports the three best candidate designs.

Optimization Constraints

The following constraints are required to be satisfied for all optimization algorithm.

0< H6 <= H2+H3

0< H7 <= H3

0< V9 <= V4

0< V10 <= V5+V4

The decision variables H6, H7, V9, and V10 are all greater than or equal to zero.

H6>=0; H7>=0; V9>=0, V10>=0.

Table 3.5 shows the constraint domain. This table is used in all the three optimization techniques. The feasible solution after solving the optimization formulation should be satisfied all constraints bounds.

Table 3.5 Optimization domain of input parameters

	Input Parameter	Brattice position vertical (V9)	Brattice position horizontal (H7)	Brattice width (H6)	Brattice length (V10)
Lower bound, X_{Lower}		**0**	**0**	**0**	**0**
Upper bound, X_{Upper}		**4**	**4**	**10**	**16**

So according to objective, the output parameters i.e. minimize or maximize values are used for decision support process. Decision support process based on criteria as applied to the parameter attributes using a weighted aggregate method. Decision support process is viewed as a post-processing action from the results of the MOGA, NLPQL, or Screening process.

3.4.2 Screening approach

Screening uses any goals that are defined the samples in the samples chart, but does not have any requirements concerning the number of objectives or goals defined. In screening approach, the optimization domain shown by Table 3.5 and optimization objective of Table 3.6 are used.

Table 3.6 Optimization objective for screening approach

Output Parameter -	**Velocity at dead end (V_d)**	**Net Pressure (P_d)**
Optimization Objective -	Maximize	Minimize

The **Screening** approach is used for preliminary design and can be used for no objective. Figure 3.6 shows the sample chart prepared by screening approach. Screening approach is based on Shifted Hammersley sampling method. A sample set of 1000 samples point is created which is relation between the output parameters i.e. velocity and pressure from CFD software. The sample set graph is shown in Figure 3.6.

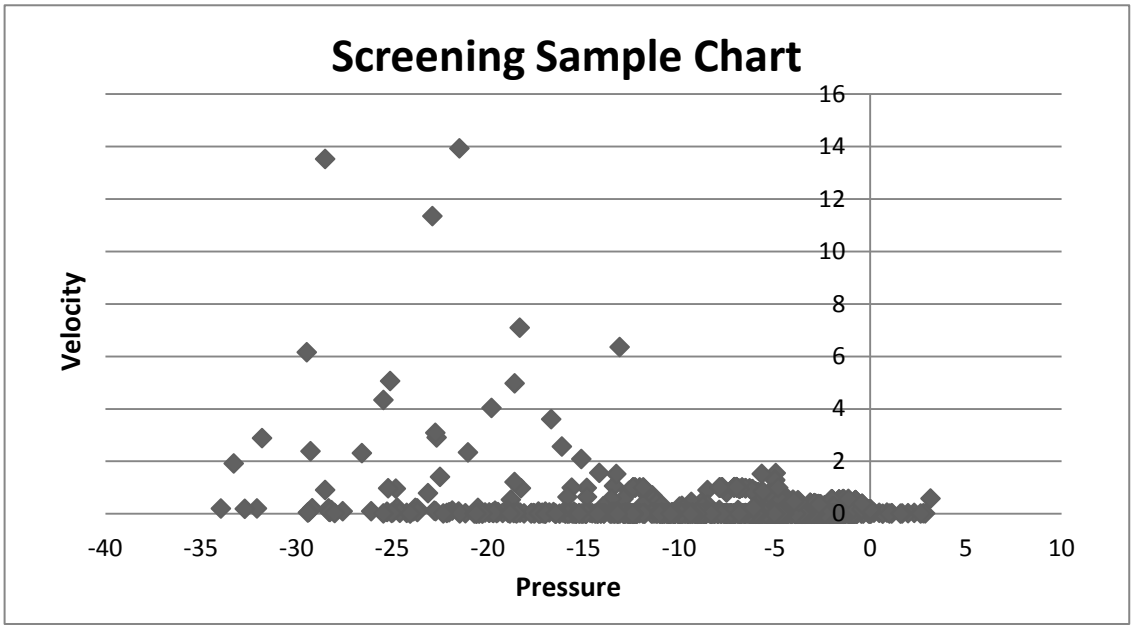

Figure 3.6 Sample chart prepared by the Screening optimization technique

3.4.3 Multi-Objective Genetic Algorithm (MOGA) approach -

MOGA requires that a goal is defined for at least one of the output parameters. Multiple output goals are allowed. In MOGA approach, the optimization domain shown in Table 3.5 and optimization objective shown in Table 3.7 are used for this study.

Table 3.7 Optimization objective for MOGA approach

Output Parameter	**Velocity at dead end (V_d)**	**Net Pressure (P_d)**
Optimization Objective	Maximize	Minimize

Figure 3.7 is representing the Pareto optimal front for the solutions of MOGA optimization. A set of 100 solution points were generated which shows the relation between the output parameters i.e. velocity and pressure from CFD analysis. The results demonstrated that the velocity of the air increases with increasing the pressure drop as expected.

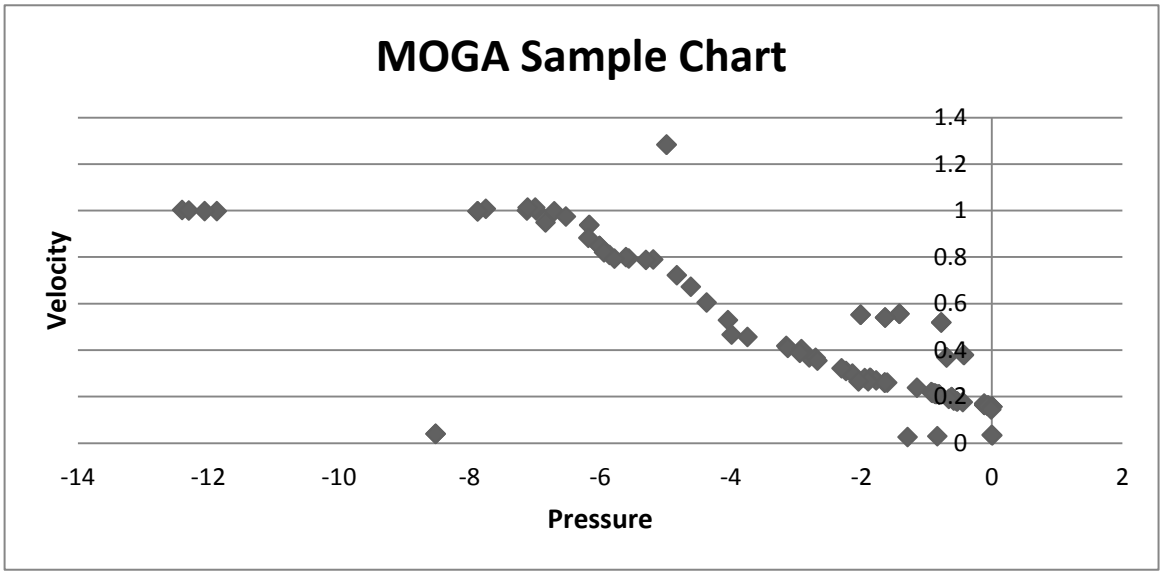

Figure 3.7 Sample chart prepared by the MOGA optimization technique

3.4.4 Non-Linear Programming by Quadratic Lagrangian (NLPQL) approach

NLPQL requires that a goal is defined for at exactly one output parameter. Only a single output goal is allowed. In NLPQL approach, the optimization domain shown by Table 3.5 and optimization objective for this approach is shown by Table 3.8. NLPQL approach is one objective oriented algorithm.

Table 3.8 Optimization objective for NLPQL approach

Output Parameter	**Net Pressure (P_d)**
Optimization Objective	Minimize

Figure 3.8 is prepared by NLPQL optimization theory. A sample set of 100 samples point which is relation between the output parameters i.e. velocity and pressure from CFD analysis. The results from NLPQL demonstrated that, same as MOGA algorithm, the velocity at the dead end increases with increasing the pressure difference. Other way, it can be conclude that to get more air, one has to crease more pressure difference between two points.

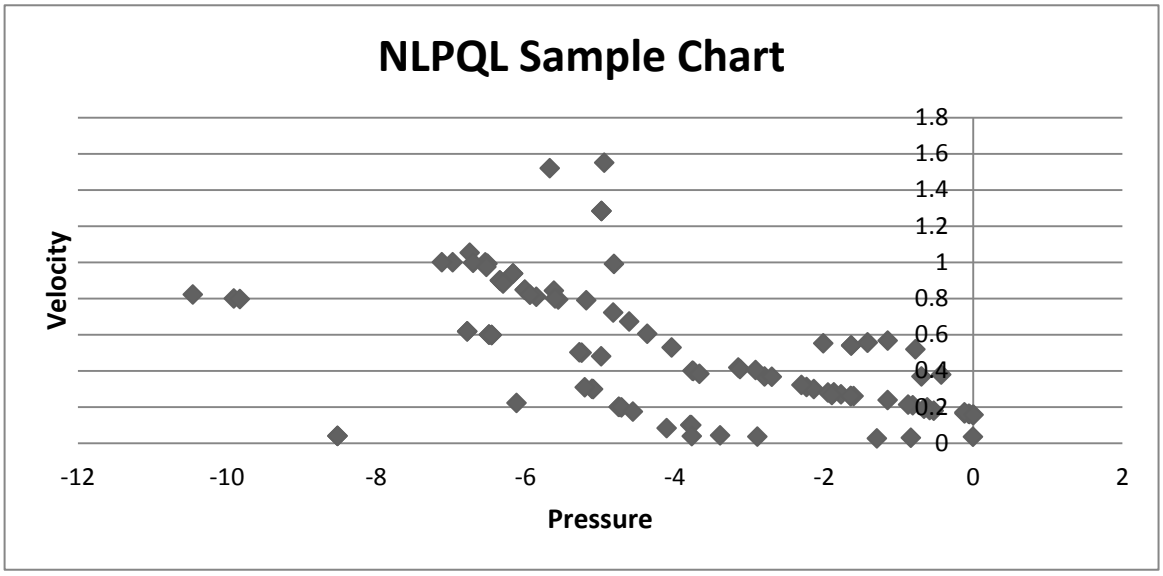

Figure 3.8 Sample chart prepared by the NLPQL optimization technique

Chapter4. Result and Discussion

4.1 Overview

The study is carried out on T-shaped crosscut region in underground mine working using CFD. CFD simulation is carried out by the ANSYS software. The quantity of air flow velocity at the dead end with two scenarios i.e. without brattice and with brattice is obtained. The effect of velocity magnitude with respect to the position of crosscut region and effect on velocity at dead end with respect to the individual input parameter is also obtained.

4.2 Solution

The discretized conservation equations are solved iteratively until convergence. Solution is performed with the optimization for different scenarios.

4.3 Simulation Results

Case (1): With no brattice

In case (1), the T-shaped crosscut region with no brattice is considered. The air is entered from the left corner with an inlet test velocity of 2 m/s. The fluid or air moves from left to right. Figure 4.1 and 4.2 shows the simulation result of velocity and pressure contour respectively.

As shown in Figure 4.1, the velocity at dead end is much less because high quanity of air passes to the outlet section because there is no obstacle on the way of air flow and air flows straight from inlet to outlet. Velocity varies near the corners of crosscut region, it is due to sudden change in geometry of crosscut region.

Air flows from high pressure to low pressure, so pressure at inlet section is more than the outlet section as shown in Figure 4.2. Pressure also varies at corners due to sudden change in geometry. There is also reversible flow occurs.

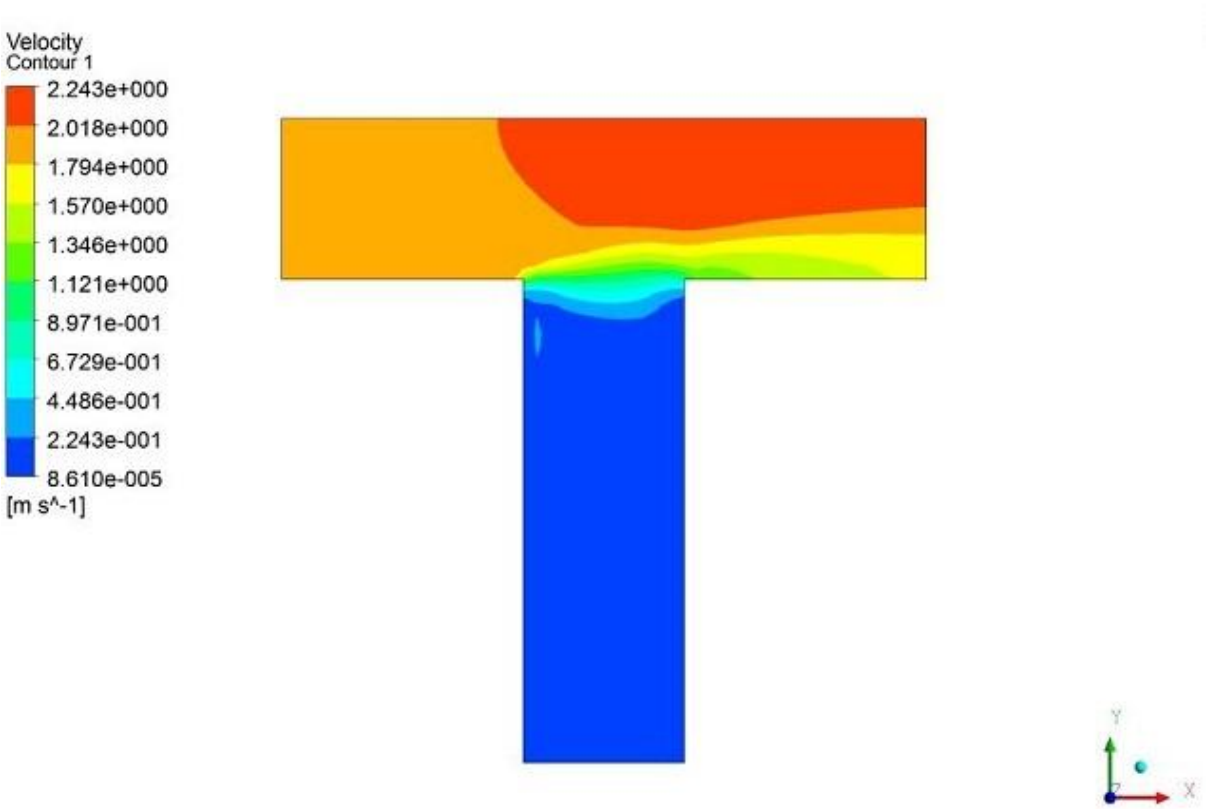

Figure 4.1 Velocity Contour of T-shaped crosscut region without brattice

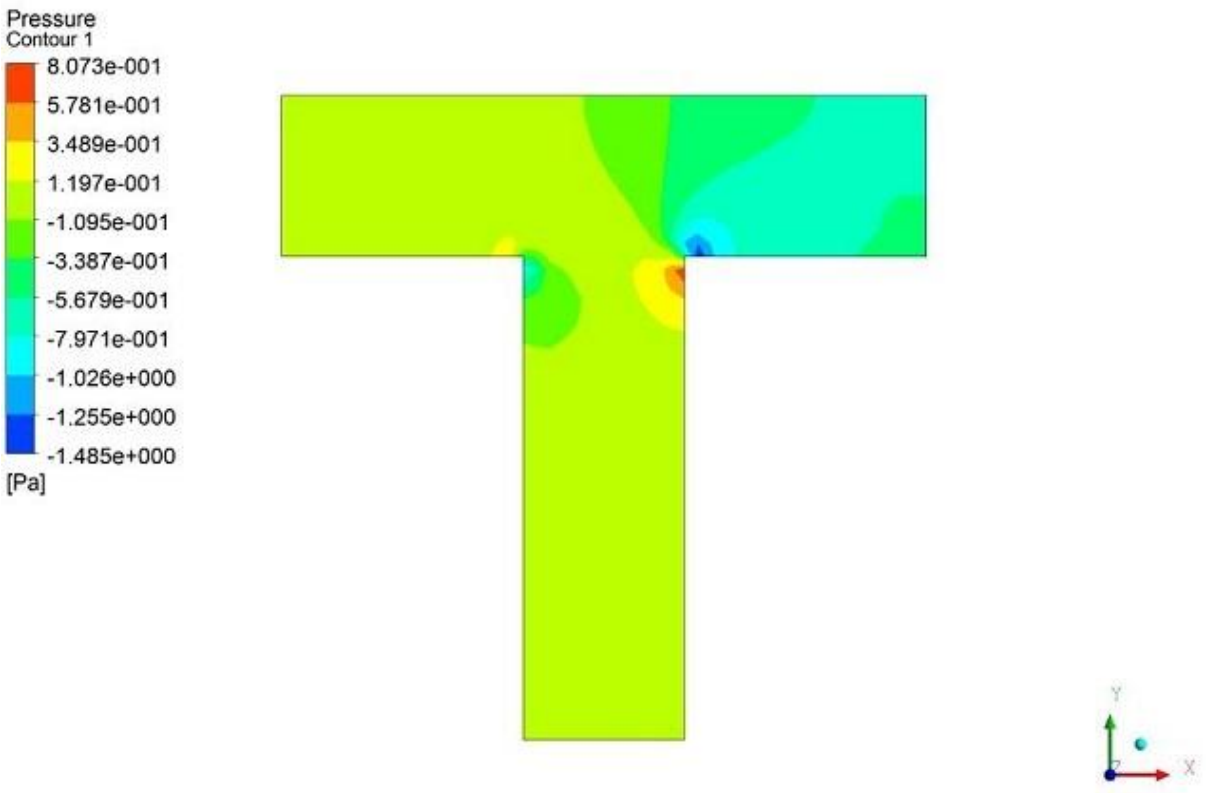

Figure 4.2 Pressure Contour of T-shaped crosscut region without brattice

The results demonstrated that the air velocity at the dead end or working face is 0.00035 m/s and pressure in crosscut region is -0.1375 Pa. Table 4.1 shows the result in case of crosscut region with no brattice.

Table 4.1 Final result in case of crosscut region with no brattice

	Velocity at dead end (V_d)	**Pressure drop (P_d)**
Final result	0.00035 m/s	-0.1375 Pa

Percentage of air speed at dead end to inlet velocity:-

$= (v_d/v_i)*100\ \%$

$= (0.00035/2)*100\ \%$

$= .0175\ \%$

Where, v_d and v_i are the velocities for the dead end and inlet test velocity respectively.

For safety and health purpose, level of minimum reaching air velocity to the workers in underground mine should be one order magnitude lower than the inlet velocity.

The main objective of mine ventilation is to increase the velocity at dead end or working face in crosscut region. In this experiment, a thin brattice in T-shaped crosscut region is included to aid or to increase the air velocity.

Case (2): With thin brattice

In case (2), the T-shaped crosscut region with brattice is considered. The air is entered from the left corner with an inlet test velocity of 2m/s. The fluid or air moves from left to right. Figure 4.3 and 4.4 shows the simulation result of velocity and pressure contour with the addition of a thin brattice in crosscut region respectively.

As shown in Figure 4.3, velocity changes at the edge of brattice because the brattice works as the obstacle for the air and when air strikes on brattice then velocity varies. At the above of

brattice, velocity of the air is much high than the inlet velocity. Velocity is increased near the brattice wall and it continues to dead end.

As shown in Figure 4.4, pressure at dead end and outlet is different from the inlet pressure. Air flows from high to low pressure so pressure at inlet section is higher than the dead end pressure and dead end pressure is higher than the outlet pressure. Below the brattice wall corner, pressure is higher than the inlet section due to reversible flow because due to high velocity, a high amount of air is reversed and pressure is incresed rapidly.

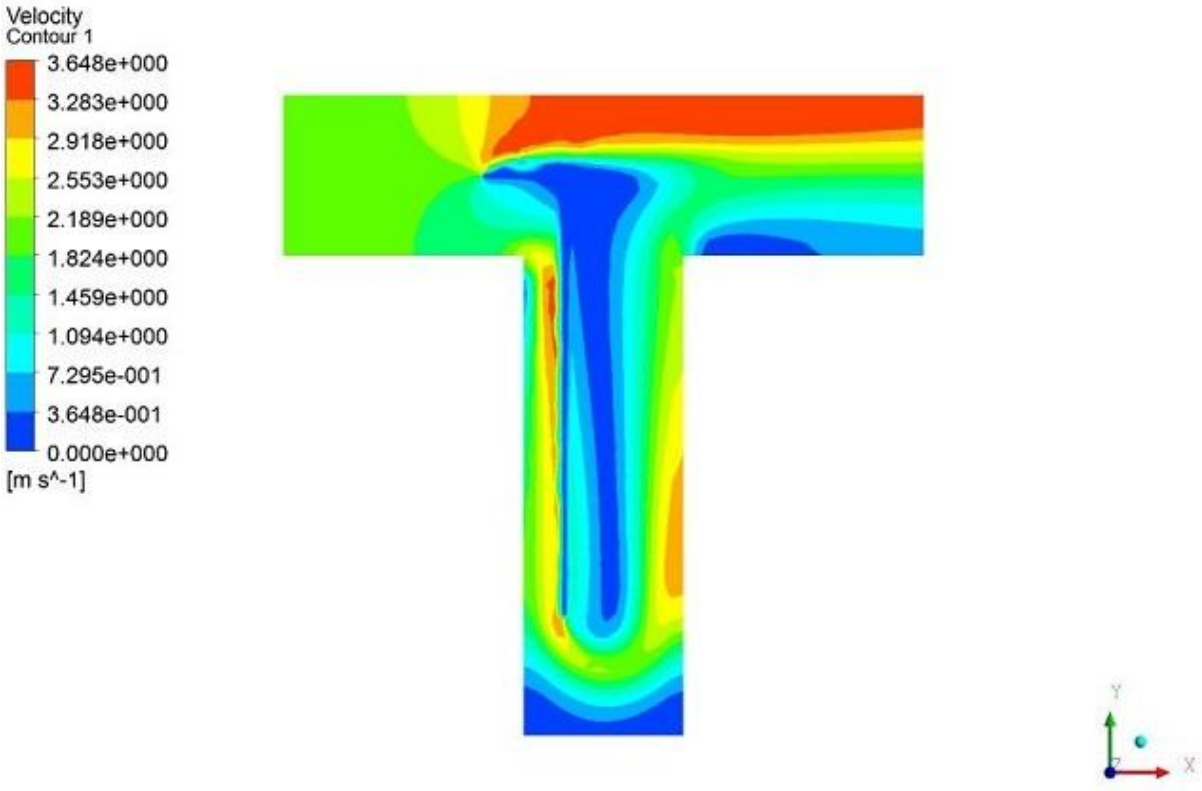

Figure 4.3 Velocity Contour of T-shaped crosscut region with thin brattice

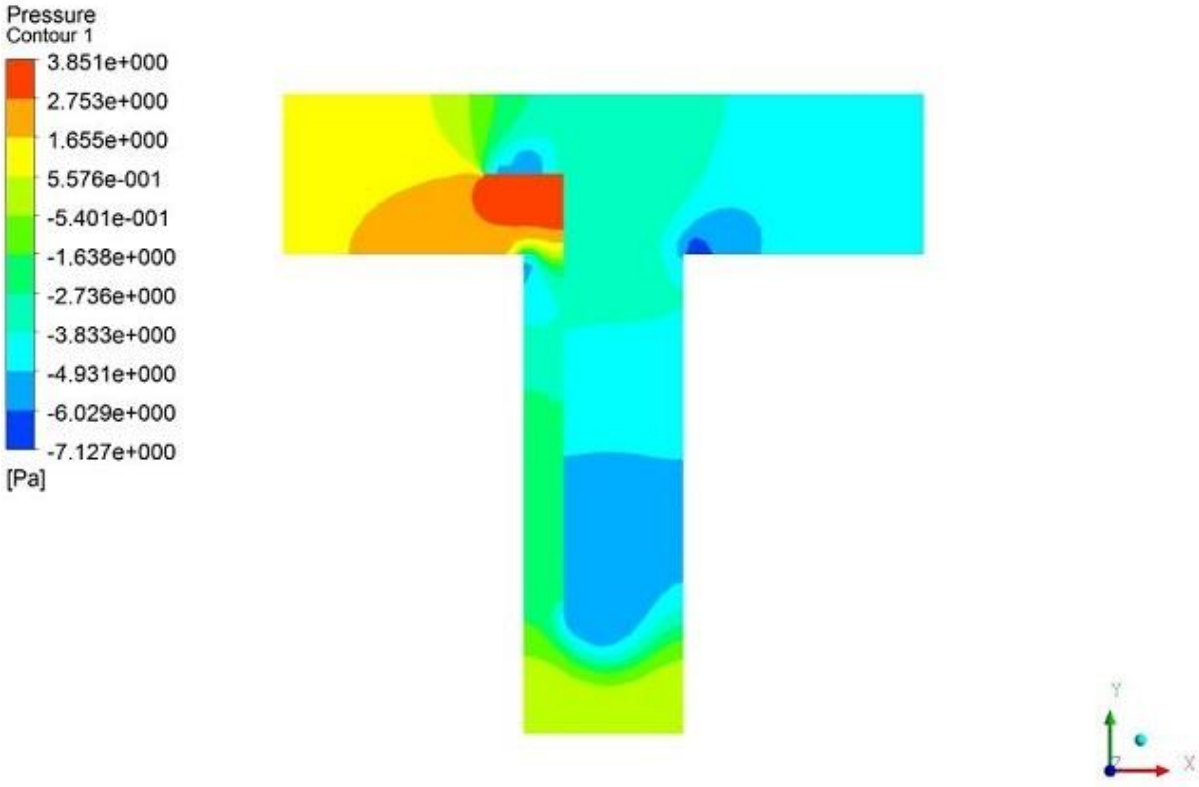

Figure 4.4 Pressure Contour of T-shaped crosscut region with thin brattice

In this experiment, air velocity at the dead end or working face is 0.12983 m/s and pressure in crosscut region is -2.5009 Pa. Table 4.2 shows the result in case of crosscut region with brattice.

Table 4.2 Final result in case of crosscut region with brattice

	Brattice position vertical	**Brattice Position horizontal**	**Brattice width**	**Brattice length**	**Velocity at dead end (V_d)**	**Pressure drop (P_d)**
Final result	2 m	1 m	2 m	11 m	0.12983 m/s	-2.5009 Pa

Percentage of air speed at dead end to inlet velocity:-

$= (v_d/v_i)*100\ \%$

$= (0.12983/2)*100\ \%$

= 6.4915 %

where, v_d and v_i are the velocities for the dead end and inlet test velocity respectively

The speed of air flow at dead end has increased 0.175% to 6.4915% with the addition of a thin brattice. The addition of brattice appears some recirculation in crosscut region. Recirculation is as the purpose of airflow is to wash out air filled with methane, dust or other gases and to supply fresh air continuously.

Case (3): With thin brattice by MOGA optimization

In case (3), the T-shaped crosscut region with brattice is considered and optimized using MOGA optimization technique to get best result. The air is entered from the left corner with an inlet test velocity of 2m/s. The fluid or air moves from left to right. Figure 4.5 and 4.6 shows the best result of simulation of velocity and pressure contour with the addition of a thin brattice in crosscut region by Multi-Objective Genetic Algorithm (MOGA) respectively.

As shown in Figure 4.5, velocity is much higher than the case (2) with brattice because the position of brattice, high quantity of air reaches at dead end due to higher pressure. Pressure at inlet section is higher than the dead end pressure and dead end pressure is higher than the outlet pressure as shown in Figure 4.6.

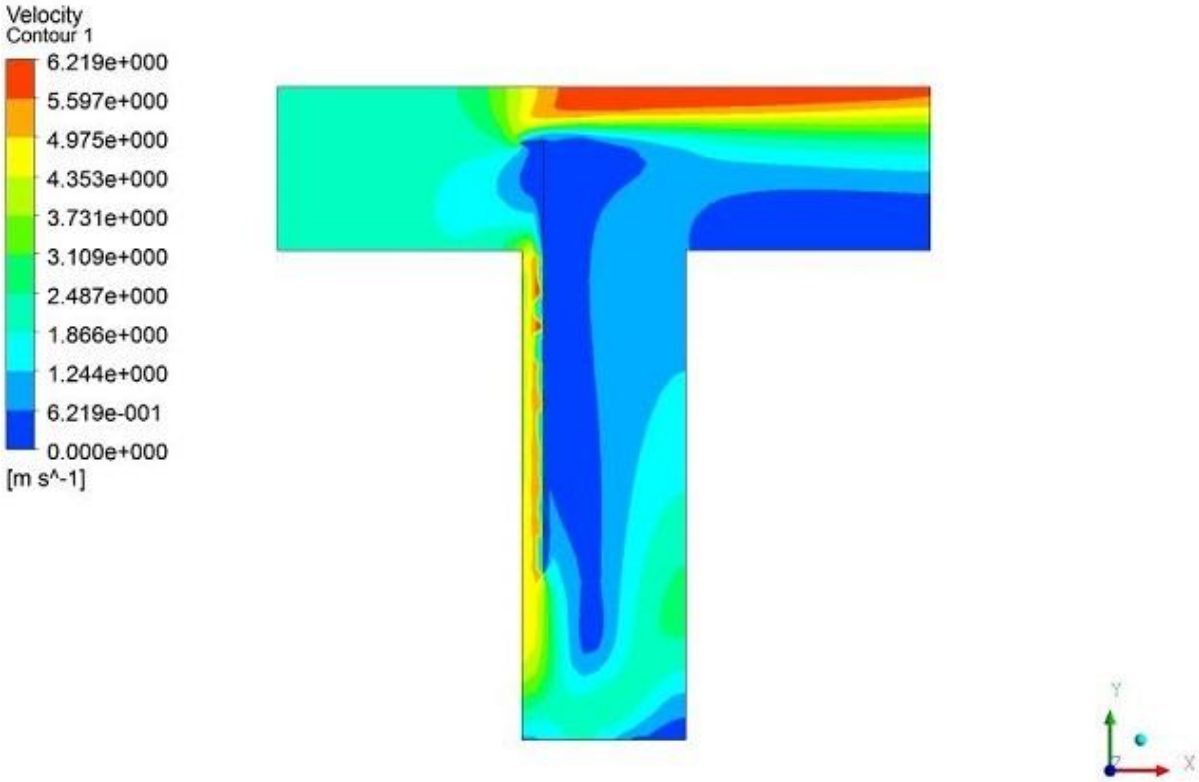

Figure 4.5 Velocity Contour of T-shaped crosscut region with thin brattice by MOGA optimization

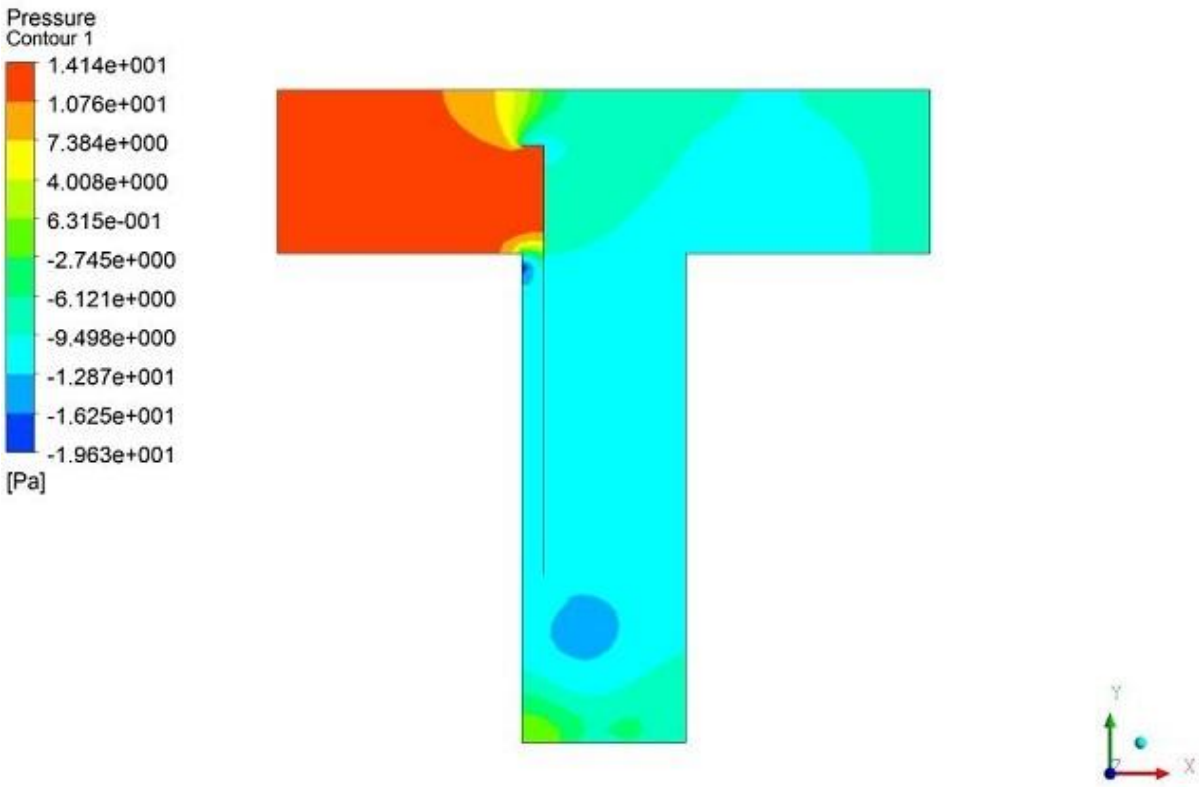

Figure 4.6 Pressure Contour of T-shaped crosscut region with thin brattice by MOGA optimization

In this experiment, air velocity at the dead end or working face is 1.2834 m/s and pressure in crosscut region is -4.9821 Pa. The air flow or air velocity at dead end as well as inside the crosscut region has more increased than the case (2) result. This is the best result from MOGA algorithm.

After the optimization, the optimized result for the best parameters of brattice which is position and dimension of brattice in T-shaped cross-cut region is obtained. Table 4.3 shows the optimized result by MOGA optimization technique.

Table 4.3 Optimized result by MOGA approach

	Brattice position vertical	**Brattice Position horizontal**	**Brattice width**	**Brattice length**	**Velocity at dead end (V_d)**	**Pressure drop (P_d)**
Optimized result	2.625 m	0.533 m	0.588 m	10.488m	1.2834 m/s	-4.9821 Pa

To get the maximum velocity at dead end, MOGA optimization technique results show that the brattice should be placed at the location presented in Table 4.3. The best location of brattice is achieved i.e. brattice position vertical and horizontal and dimension of brattice i.e. width and length of brattice by MOGA.

Percentage of air speed at dead end to inlet velocity:-

$= (v_d/v_i)*100\ \%$

$= (1.2834/2)*100\ \%$

$= 64.17\ \%$

where, v_d and v_i are the velocities for the dead end and inlet test velocity respectively

The speed of air flow at dead end has increased from 6.4915% to 64.17% with the addition of a thin brattice and with thin brattice by MOGA respectively. In this result, the optimize result i.e. maximum velocity at dead end with minimum pressure drop was obtained by MOGA optimization technique.

Case (4): With thin brattice by NLPQL optimization

In case (4), the T-shaped crosscut region with brattice is considered with NLPQL optimization technique. The air is entered from the left corner with an inlet test velocity of 2m/s. The fluid or air moves from left to right. Figure 4.7 and 4.8 shows the best result of simulation of velocity and pressure contour with the addition of a thin brattice in crosscut region using Non-Linear Programming by Quadratic Lagrangian (NLPQL) algorithm.

As shown in Figure 4.7, velocity is much higher than the other cases because the position and dimension of brattice, high quantity of air reaches at dead end due to higher pressure. Pressure at inlet section is higher than the dead end pressure and dead end pressure is higher than the outlet pressure shown in Figure 4.8. Due to reversible flow, velocity and pressure varies inside the crosscut region from high to low and low to high.

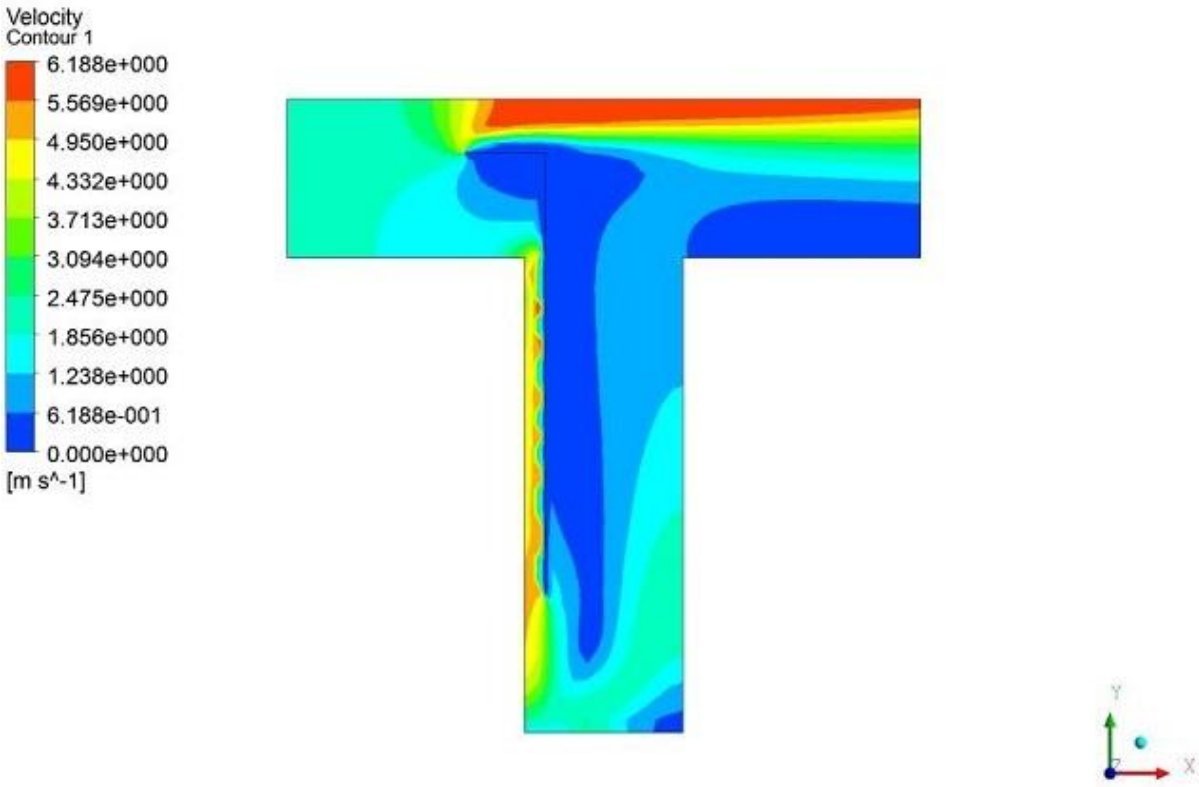

Figure 4.7 Velocity Contour of T-shaped crosscut region with thin brattice by NLPQL optimization

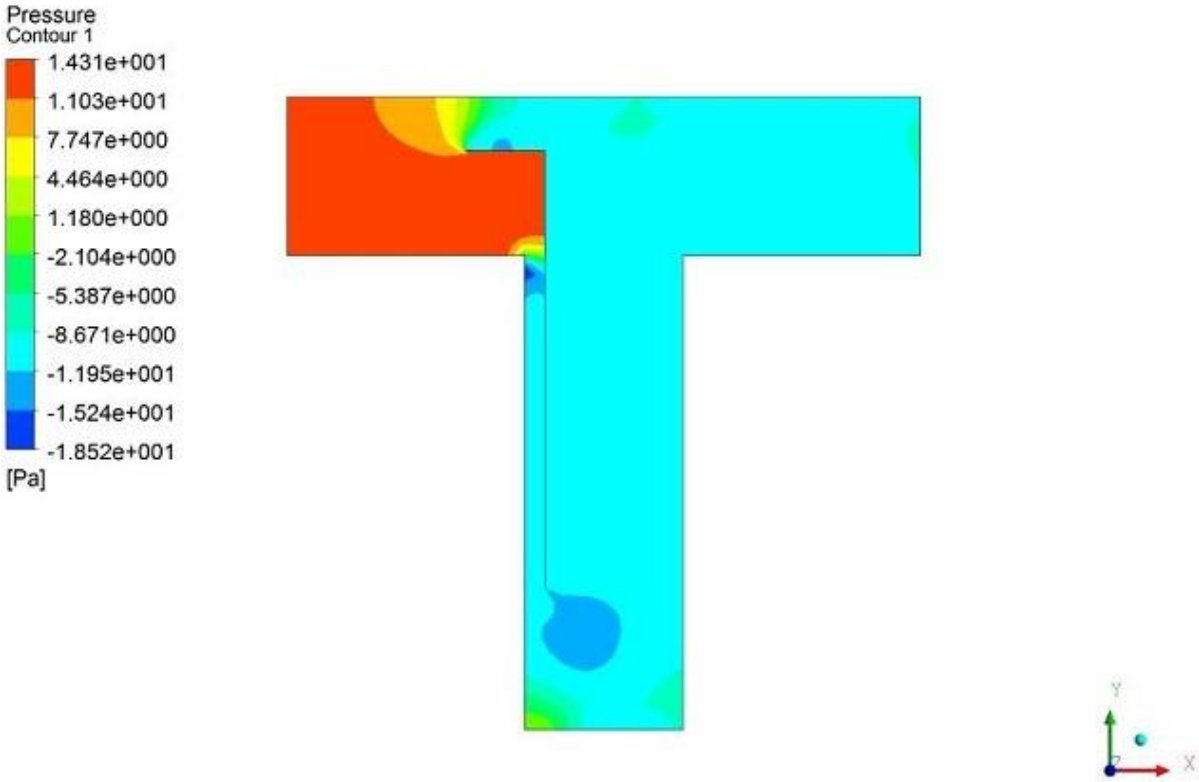

Figure 4.8 Pressure Contour of T-shaped crosscut region with thin brattice by NLPQL optimization

In this experiment, air velocity at the dead end or working face is 1.551 m/s and pressure in crosscut region is -4.9448 Pa. The air flow or air velocity at dead end as well as inside the crosscut region has more increased than the case (2). This is the best result from NLPQL algorithm.

After the optimization, the optimized result for the best parameters of brattice is obtained which is position and dimension of brattice in T-shaped cross-cut region. Table 4.4 shows the optimized result by NLPQL optimization technique.

Table 4.4 Optimized result by NLPQL approach

	Brattice position vertical	**Brattice Position horizontal**	**Brattice width**	**Brattice length**	**Velocity at dead end (V_d)**	**Pressure drop (P_d)**
Optimized result	2.652 m	0.501 m	2 m	11.061 m	1.551 m/s	-4.9488 Pa

The best location of brattice is obtained by NLPQL i.e. brattice position vertical and horizontal and dimension of brattice i.e. width and length of brattice to achieve minimum pressure drop.

Percentage of air speed at dead end to inlet velocity:-

$= (v_d/v_i)*100\ \%$

$= (1.551/2)*100\ \%$

$= 77.55\ \%$

where, v_d and v_i are the velocities for the dead end and inlet test velocity respectively

The speed of air flow at dead end has increased from 6.4915% to 77.55% with the addition of a thin brattice and with thin brattice by NLPQL respectively. In this result, the optimize result i.e. minimum pressure drop by NLPQL optimization technique is achieved.

4.4 Correlation between Input parameters and velocity

In this section of result, the relationship between the input parameters and dead end velocity was established. The four input parameters for optimization were considered i.e. brattice position vertical and horizontal, width and length of brattice. Optimization is performed only in the case of crosscut region with brattice. So this section includes the response of velocity at dead end with respect to the different input parameters.

Brattice position vertical v/s Velocity

Figure 4.9 shows that as increasing the vertical brattice position, velocity at dead end or working face also increases. As increasing the vertical position, quantity of air increases through the brattice wall and high velocity reaches at dead end because air quantity reaches at outlet is less and vice-versa.

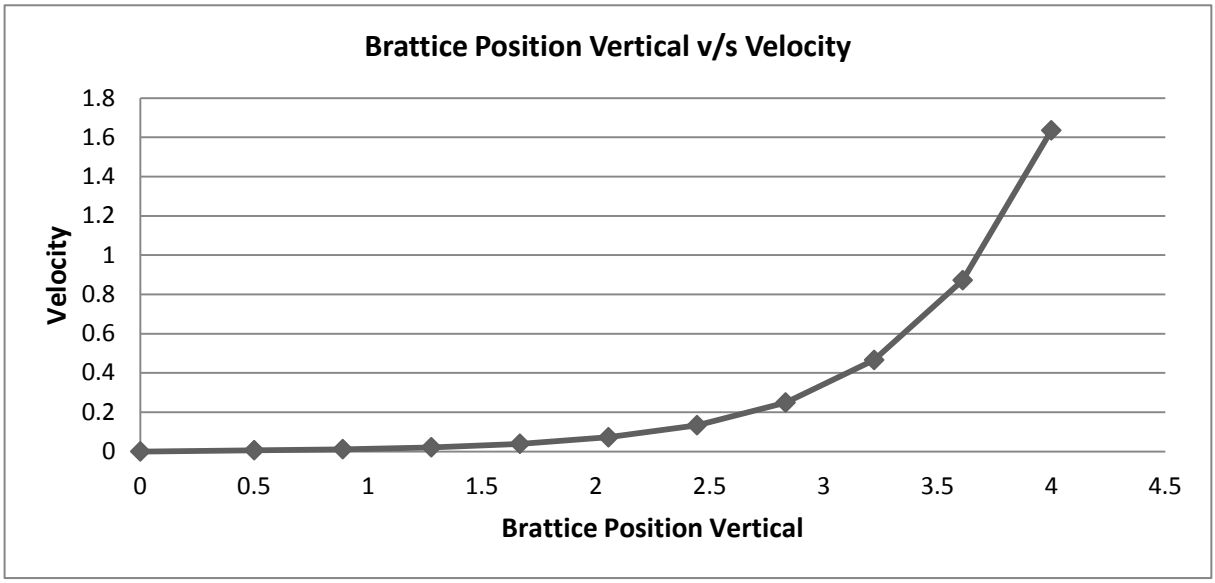

Figure 4.9 Relation between Brattice position vertical and Velocity

Brattice position horizontal v/s Velocity

Figure 4.10 shows that as increasing the horizontal brattice position, velocity at dead end or working face decreases except at very initial. At zero dimension of horizontal brattice position, velocity at dead end also is same as the velocity that in case of no brattice because there is no way to reach air at dead end. After increasing horizontal position of brattice from zero, velocity at dead end increases rapidly because high velocity reaches at dead end through the brattice wall. As increasing the horizontal position, the distance between brattice and air hit position on brattice increases so the quantity of air decreases through the brattice wall and reaches less air quantity.

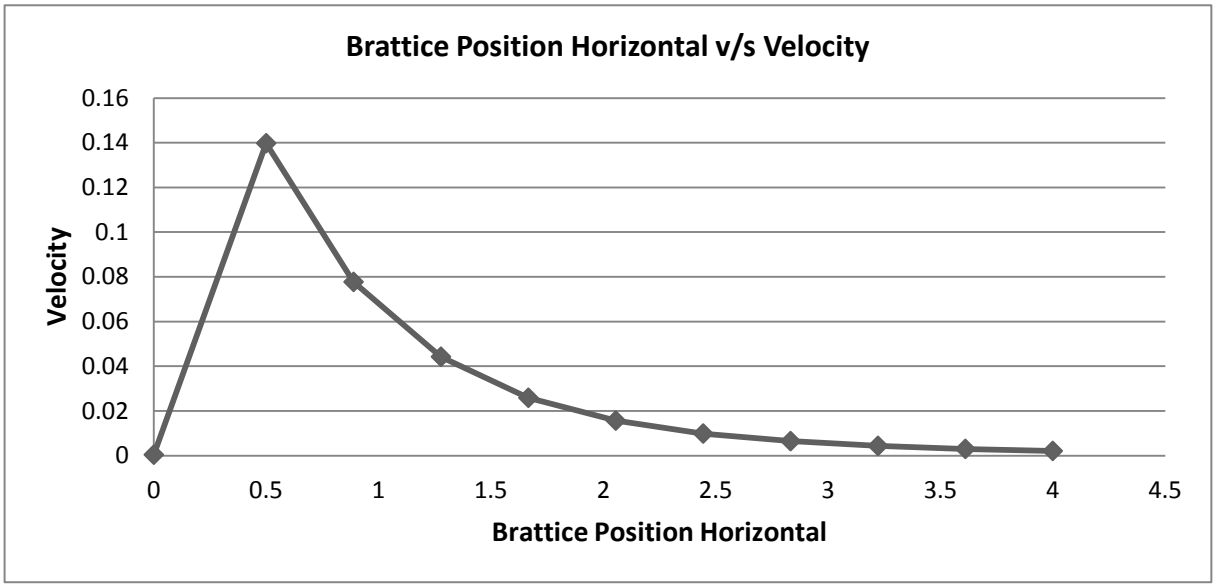

Figure 4.10 Relation between Brattice position horizontal and Velocity

Brattice width v/s Velocity

Figure 4.11 shows that as increasing the brattice width, velocity at dead end working face remains same. There is no effect of brattice width on velocity at dead end. There is no point to hit velocity on brattice width because it is horizontal with respect to the air flow so will be no effect on air quantity at dead end and remains same as the case of brattice.

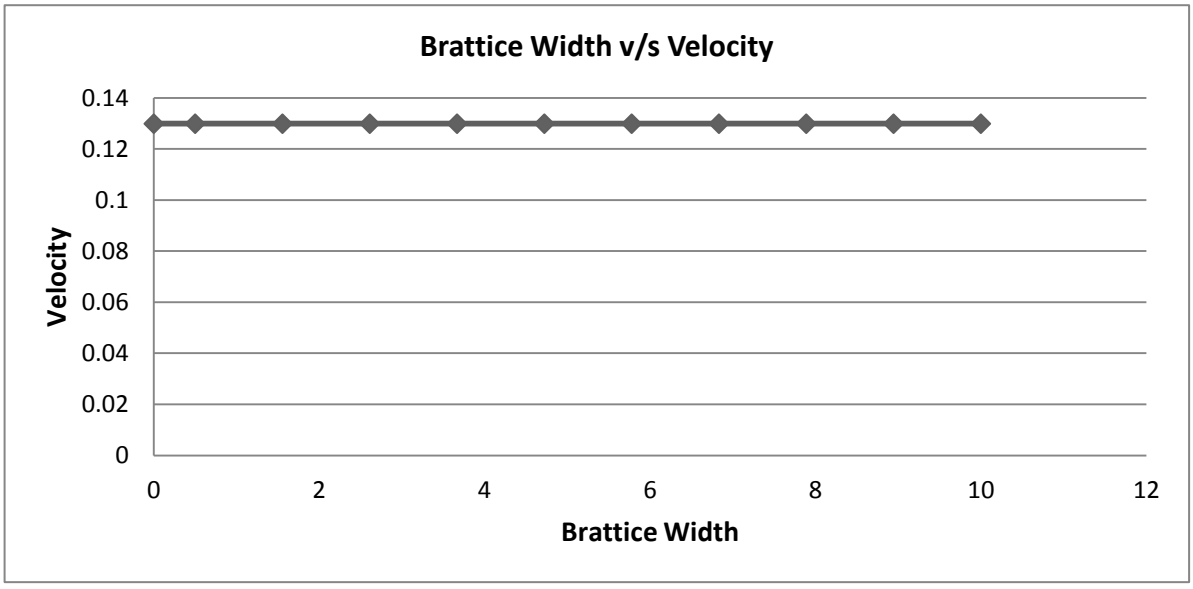

Figure 4.11 Relation between Brattice width and Velocity

Brattice length v/s Velocity

Figure 4.12 shows that as increasing the brattice length, velocity at dead end working face also increases. The lower portion of brattice is near the dead end so as increasing the length, air quantity would be increases through the brattice wall at dead end and if brattice length decreases then quantity of air would be less at dead end.

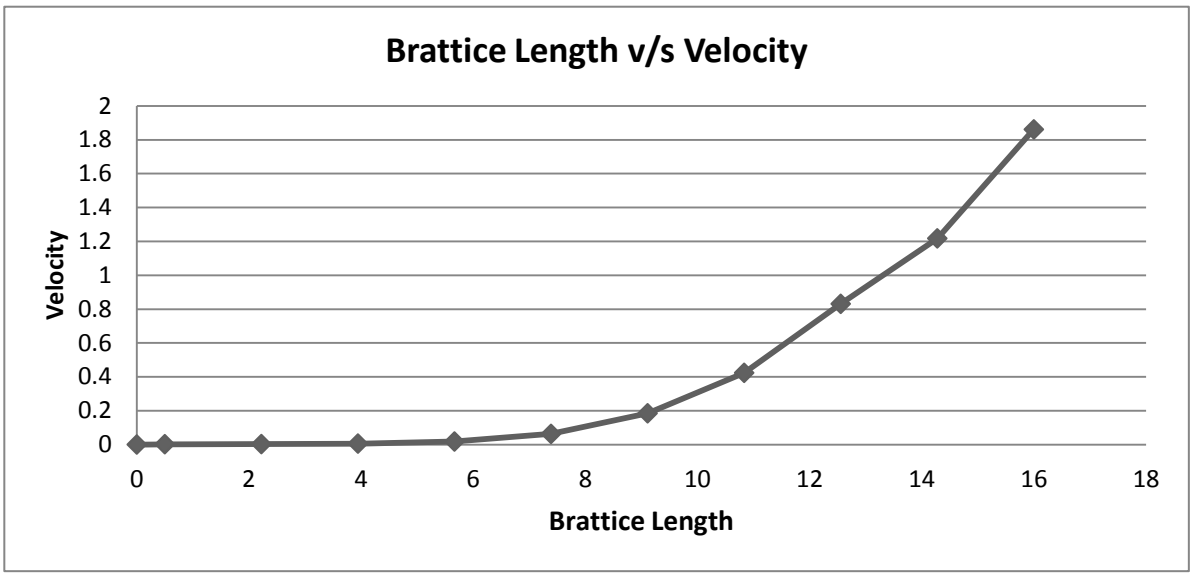

Figure 4.12 Relation between Brattice length and Velocity

Chapter5. Conclusion

5.1 Conclusion

A computational fluid dynamic study is conceded to achieve maximum velocity at dead end or working face in a T-shaped crosscut region. Spalart-Allmaras turbulent model is used for CFD analysis. There are two optimization techniques are used to optimize the parameters to achieve best result. In this experiment, a thin brattice is the most effective for simulating the velocity at dead zone inside the crosscut region. A thin brattice is also more space efficient. An addition of a thin brattice helps in diverting the air flow in crosscut region. The optimized result of air flow at dead end in crosscut region is 65-75% of the original case of no brattice. The optimized result of input parameters i.e. location and dimension of brattice aid to maximize the air flow velocity at dead end and minimize the pressure inside the crosscut region. It is found that between the two optimization techniques, the result that is velocity at dead end and keep pressure is minimized in T-shaped crosscut region by NLPQL optimization approach is better than the MOGA optimization approach.

Chapter6. References

6.1 References

1. Amano, K., Sakai, K., & Mizuta, Y., A calculation system using a personal computer for the design of underground ventilation and air conditioning. Mining Science and Technology, 4(2), (1987): pp. 193-208.
2. Aminossadati, S. M., & Hooman, K., Numerical simulation of ventilation air flow in underground mine workings. In 12th US/North American Mine Ventilation Symposium (2008): pp. 253-259.
3. Kurnia, J. C., Sasmito, A. P., & Mujumdar, A. S., CFD Simulation of Methane Dispersion and Innovative Methane Management in Underground Mining Faces. Applied Mathematical Modelling (2014).
4. Chanteloup, V., & Mirade, P. S., Computational fluid dynamics (CFD) modelling of local mean age of air distribution in forced-ventilation food plants. Journal of food engineering, 90(1), (2009): pp. 90-103.
5. Toraño, J., Torno, S., Menéndez, M., & Gent, M., Auxiliary ventilation in mining roadways driven with roadheaders: Validated CFD modelling of dust behaviour. Tunnelling and Underground Space Technology, 26(1), (2011): pp. 201-210.
6. Diego, I., Torno, S., Toraño, J., Menéndez, M., & Gent, M., A practical use of CFD for ventilation of underground works. Tunnelling and Underground Space Technology, 26(1), (2011): pp. 189-200.
7. Xu, G., Luxbacher, K. D., Ragab, S., & Schafrik, S., Development of a remote analysis method for underground ventilation systems using tracer gas and CFD in a simplified laboratory apparatus. Tunnelling and Underground Space Technology, 33, (2013): pp. 1-11.
8. Sasmito, A. P., Birgersson, E., Ly, H. C., & Mujumdar, A. S., Some approaches to improve ventilation system in underground coal mines environment–A computational fluid dynamic study. Tunnelling and Underground Space Technology, 34, (2013): pp. 82-95.
9. Torno, S., Toraño, J., Ulecia, M., & Allende, C., Conventional and numerical models of blasting gas behaviour in auxiliary ventilation of mining headings. Tunnelling and Underground Space Technology, 34, (2013): pp. 73-81.
10. Ren, T., Wang, Z., & Cooper, G., CFD modelling of ventilation and dust flow behaviour above an underground bin and the design of an innovative dust mitigation system. Tunnelling and Underground Space Technology, 41, (2014): pp. 241-254.

11. Kurnia, J. C., Sasmito, A. P., & Mujumdar, A. S., Simulation of a novel intermittent ventilation system for underground mines. Tunnelling and Underground Space Technology, 42, (2014): pp. 206-215.
12. Guo, X., & Zhang, Q., Analytical solution, experimental data and CFD simulation for longitudinal tunnel fire ventilation. Tunnelling and Underground Space Technology, 42, (2014): pp. 307-313.
13. Torano, J., Torno, S., Menéndez, M., & Gent, M., Auxiliary ventilation in mining roadways driven with roadheaders: Validated CFD modelling of dust behaviour. Tunnelling and Underground Space Technology, 26(1), (2011): pp. 201-210.
14. Likar, J., & Čadež, J., Ventilation design of enclosed underground structures. Tunnelling and Underground Space Technology, 15(4), (2000): pp. 477-480.
15. Lowndes, I. S., Crossley, A. J., & Yang, Z. Y., The ventilation and climate modelling of rapid development tunnel drivages. Tunnelling and underground space technology, 19(2), (2004): pp. 139-150
16. Parra, M. T., Villafruela, J. M., Castro, F., & Mendez, C., Numerical and experimental analysis of different ventilation systems in deep mines. Building and Environment, 41(2), (2006): pp. 87-93.
17. Torano, J., Torno, S., Menendez, M., Gent, M., & Velasco, J., Models of methane behaviour in auxiliary ventilation of underground coal mining. International Journal of Coal Geology, 80(1), (2009): pp. 35-43.
18. Ghosh, S.K., Ranjan, M., and Kumar, K., Mine ventilation in a bord and pillar mines using cfd. International Journal of Emerging Technology and Advanced Engineering, Volume 3, (2013): pp. 389-393.
19. Hargreaves, D. M., & Lowndes, I. S., The computational modeling of the ventilation flows within a rapid development drivage. Tunnelling and underground space technology, 22(2), (2007): pp. 150-160.
20. Su, S., Chen, H., Teakle, P., & Xue, S., Characteristics of coal mine ventilation air flows. Journal of environmental management, 86(1), (2008): pp. 44-62.
21. Liu, G. N., Gao, F., Ji, M., & Liu, X. G., Investigation of the ventilation simulation model in mine based on multiphase flow. Procedia Earth and Planetary Science, 1(1), (2009): pp. 491-496.
22. Colella, F., Rein, G., Verda, V., & Borchiellini, R., Multiscale modeling of transient flows from fire and ventilation in long tunnels. Computers & Fluids, 51(1), (2011): pp. 16-29.

23. Amano, K., Sakai, K., & Mizuta, Y., A calculation system using a personal computer for the design of underground ventilation and air conditioning. Mining Science and Technology, 4(2), (1987): pp. 193-208.
24. Noack, K., Control of gas emissions in underground coal mines. International Journal of Coal Geology, 35(1), (1998): pp. 57-82.
25. Kissell, F. N., & Matta, J. E., U.S. Patent No. 4,157,204. Washington, DC: U.S. Patent and Trademark Office. (1979).